Journal of Medicinal Chemistry

ARTICLE

pubs.acs.org/jmc

Synthesis and Antiangiogenic Activity of New Silybin Galloyl Esters

Radek Gažák,[†] Kateřina Valentová,[‡] Kateřina Fuksová,[†] Petr Marhol,[†] Marek Kuzma,[†] Miguel Ángel Medina,[§] Ivana Oborná,[∥] Jitka Ulrichová,[‡] and Vladimír Křen*[,†]

[†]Centre of Biotransformation and Biocatalysis, Institute of Microbiology Academy of Sciences of the Czech Republic, Vídeňská 1083, Prague 4, CZ 142 20, Czech Republic

[‡]Department of Medical Chemistry and Biochemistry, Faculty of Medicine and Dentistry, Palacký University, Hněvotínská 3, CZ-775 15 Olomouc, Czech Republic

[§]Department of Molecular Biology and Biochemistry, University of Málaga, Campus de Teatinos, ES 29071 Málaga, Spain

[∥]Department of Obstetrics and Gynecology, Faculty of Medicine and Dentistry, Palacký University and University Hospital in Olomouc, I. P. Pavlova 6, 775 20 Olomouc, Czech Republic

Supporting Information

ABSTRACT: The synthesis of various silybin monogalloyl esters was developed, and their antiangiogenic activities were evaluated in a variety of in vitro tests with human umbilical vein endothelial cells (HUVECs). A structure−activity relationship (SAR) study found the regioselectivity of the silybin galloylation to be highly significant. Silybin (as an equimolar mixture of two diastereomers A and B) exhibited quite poor antiangiogenic activities, whereas its B stereoisomer is more active than silybin A. The galloylation of phenolic OH groups of natural silybin (a mixture of both isomers) leads to increases in their antiangiogenic activities, which is more apparent with the 7-OH than the 20-OH. In contrast, gallates at aliphatic OH groups either had a comparable activity to the parent compound or are even worse than silybin, which was observed in the case of 3-*O*-galloylsilybin. The most effective compound from this series (7-*O*-galloylsilybin) has also been prepared from stereochemically pure silybins A and B to evaluate the effect of stereochemistry on the activity. As with silybin itself, the B isomer of 7-*O*-galloylsilybin was more active than the A isomer.

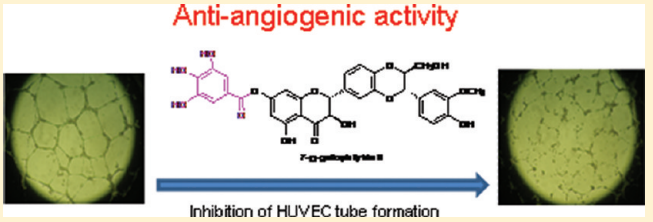

INTRODUCTION

The flavonolignan silybin (**1**), a natural polyphenol contained in the milk thistle (*Silybum marianum*) extract (so-called silymarin), is a well-known flavonoid possessing multiple biological activities at various cell levels.[1] This compound is attracting increasing attention, which is also reflected in a high number of papers published recently[1] (e.g., 204 papers in 2010; ISI, Web of Science).

Natural silybin consists of an approximately equimolar mixture of two diastereomers, silybin A (**1a**) and silybin B (**1b**) (Figure 1), whose absolute configuration has been determined recently.[2,3] Their analytical separation is feasible using reverse-phase HPLC,[4,5] but preparative separation is extremely complicated. It was satisfactorily achieved by ourselves quite recently using lipases.[6,7]

Silybin is an active component in a plethora of phytopreparations used for the prevention and treatment of some liver diseases and as an antidote against a number of hepatotoxins and mycotoxins. The antioxidant and antiradical activities of silybin have been studied, and respective molecular mechanisms were described in detail.[8,9] Recently, intravenous silybin was successfully used for the effective retreatment of HIV−HCV (HCV = chronic hepatitis C virus) co-infected patients who did not respond to pegylated interferon plus ribavirin combination therapy with high anti-HCV efficacy, a decrease in HIV replication, and increase in $CD4^+$ cells.[10]

Studies in approximately the past 20 years have shown that silybin not only is an efficient hepatoprotectant and/or antioxidant but also possesses many other advantageous activities, such as anticancer, chemopreventive, hypocholesterolemic, cardioprotective, and neuroprotective activities.[1,11] Silybin's anticancer effects were demonstrated in the treatment of some prostatic diseases including adenocarcinoma,[12] human non-small-cell lung carcinoma H1299, H460, and H322 cells,[13] and xenografts of human colorectal cancer SW480.[14] Silybin was found to be an effective anticancer compound not only in the early stages of many cancer types but also in the late phases, including metastasis,[12,15] which is difficult to treat using current commercial anticancer agents.

One of the mechanisms of silybin anticancer activity consists of its antiangiogenic effects, involving several events connected with this complex process, e.g., growth inhibition, cell cycle arrest, apoptosis induction, inhibition of capillary tube organization, reduced invasion, and migration of human endothelial cells.[16]

Received: August 2, 2011
Published: September 19, 2011

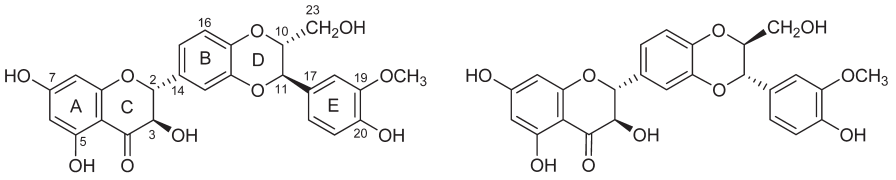

1a: silybin A (2*R*, 3*R*, 10*R*, 11*R*) **1b**: silybin B (2*R*, 3*R*, 10*S*, 11*S*)

Figure 1. Structures of silybin diastereomers.

The biological effects of optically pure silymarin components have been mostly disregarded mainly because of their difficult separation at a preparative scale. However, recent studies on the pharmacological activity of pure silybins A and B clearly demonstrated that the two silybin diastereomers **1a** and **1b** have different biological activities; e.g., **1b** has estrogenic activity, whereas **1a** exhibits no such activity.[17] A study of the anticancer efficacy of pure silymarin components on human prostate carcinoma DU145 cells demonstrated that isosilybin B is the most effective at suppressing the topoisomerase IIα gene promoter and silybin B has the most significant effect on the G1 cell cycle accumulation of these cancer cells.[18] Another study of pure silymarin components on advanced human prostate cancer PC3 cells showed that isosilybin B and silybin B are the most potent compounds at inhibiting cell growth and colony formation.[19] The potency of silybin B at inducing the cell death of PC3 cells was lower than that of both isosilybins; however, it was still significant and higher than that of silybin A.

The presence of a galloyl moiety in the structure of flavonoids (e.g., catechins) was found to be an important prerequisite for their significant antiangiogenic properties (typically in *epi*-gallocatechin gallate, EGCG).[20] Besides this, the introduction of a galloyl moiety is expected to also improve the antioxidant and chemoprotective activity of the resulting molecule. Therefore, the synthesis of a series of silybin galloyl esters was developed in this work with the aim of preparing new compound(s) with significant antiangiogenic activity. The most active galloyl ester of silybin was also prepared from stereochemically pure **1a** and **1b** to assess the effect of stereochemistry on antiangiogenic activity.

CHEMISTRY

The silybin molecule contains five hydroxyl groups with various properties, which makes selective silybin functionalization a difficult task. Recently, we reported a relatively complete toolbox for the selective protection/deprotection of silybin, including regioselective esterification.[21] Selective acylation of the phenolic OH group at C-7 can be achieved using the corresponding acyl chloride or anhydride in pyridine.[22] The primary alcoholic group at C-23 is another OH group that can be regioselectively esterified without the prior protection of other OH groups, using the following methods: (i) the Mitsunobu reaction (carboxylic acid, Ph_3P, and DEAD);[23] (ii) Lewis acid catalysis (acyl chloride/anhydride, $BF_3 \cdot Et_2O$);[22] (iii) biocatalytic methods using lipases (Novozym 435, carboxylic acid or vinyl ester).[7,24]

Existing methods of regioselective monoesterification of silybin were utilized for the synthesis of gallates. Only the use of acyl chloride in pyridine led to the intended monogalloylation of the silybin molecule, specifically at the 7-OH (Scheme 1). However, the regioselectivity of this reaction was not very high, which resulted in a rather low yield of the corresponding product **9** (~30%). As the 7-OH group is the most acidic group of the silybin molecule (because of the -M effect of the carbonyl at C-4), we tried to improve its regioselectivity in favor of the ester at the 7-OH by the selective generation of phenolate at this position using a relatively weak base, Et_3N. Optimizing the reaction conditions with Et_3N led to the development of a highly regioselective method for the galloylation of the 7-OH (Scheme 1).

Scheme 1. Synthesis of 7-*O*-Galloylsilybin (5)[a]

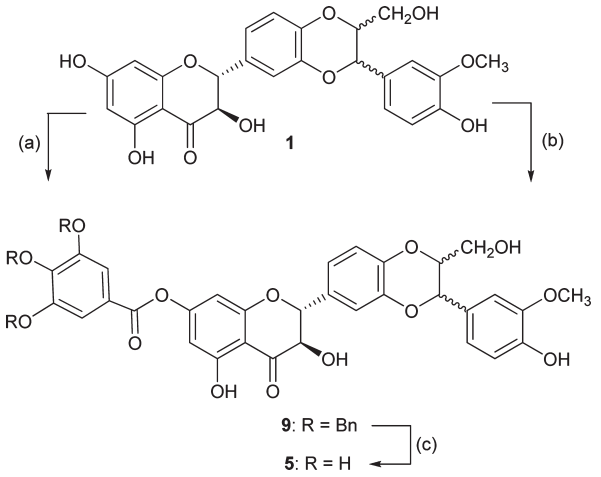

[a] Reagents and conditions: (a) 3,4,5-tri-*O*-benzylgalloyl chloride (1.2 equiv), pyridine, DMAP (1 equiv), 0 °C, 1 h, 32%; (b) 3,4,5-tri-*O*-benzylgalloyl chloride (1.2 equiv), Et_3N (2 equiv), CH_2Cl_2/MeCN (1:1), room temp, 1 h, 81%; (c) H_2—Pd/C, EtOAc, room temp, 12 h, 91%.

The galloylation of the primary 23-OH of **1** using reported chemical methods failed (Mitsunobu reaction and Lewis acid catalysis), as well as the use of lipase (Novozym 435), which is generally feasible with aliphatic acids but with aromatic acids does not proceed at all, as we found in all related previous studies[25−30] and tried ourselves without success. Therefore, to achieve monoesterification of the silybin 23-OH group, a suitable protected derivative had to be prepared before the intended esterification. The higher acidity of phenolic OH groups allows their selective alkylation in the presence of alcoholic OH groups, e.g., benzylation, which leads to an appropriate partially protected silybin derivative, 5,7,20-tri-*O*-benzylsilybin (**10**).[8] This compound still contains two free OH groups (at C-3 and C-23), but the use of benzyl- or MOM-protected gallic acid with DCC/DMAP at 0 °C leads to a selective esterification of the 23-OH (Scheme 2). On the basis of these experiments, we ascertained that the use of the MOM group for gallic acid protection (compound **4**) instead of the benzyl group considerably simplified purification of the product from the reaction mixture. The use of this orthogonal protection enabled catalytic hydrogenolysis of the crude reaction mixture after esterification and made

Scheme 2. Synthesis of 3-*O*-Galloylsilybin (7) and 23-*O*-Galloylsilybin (6)[a]

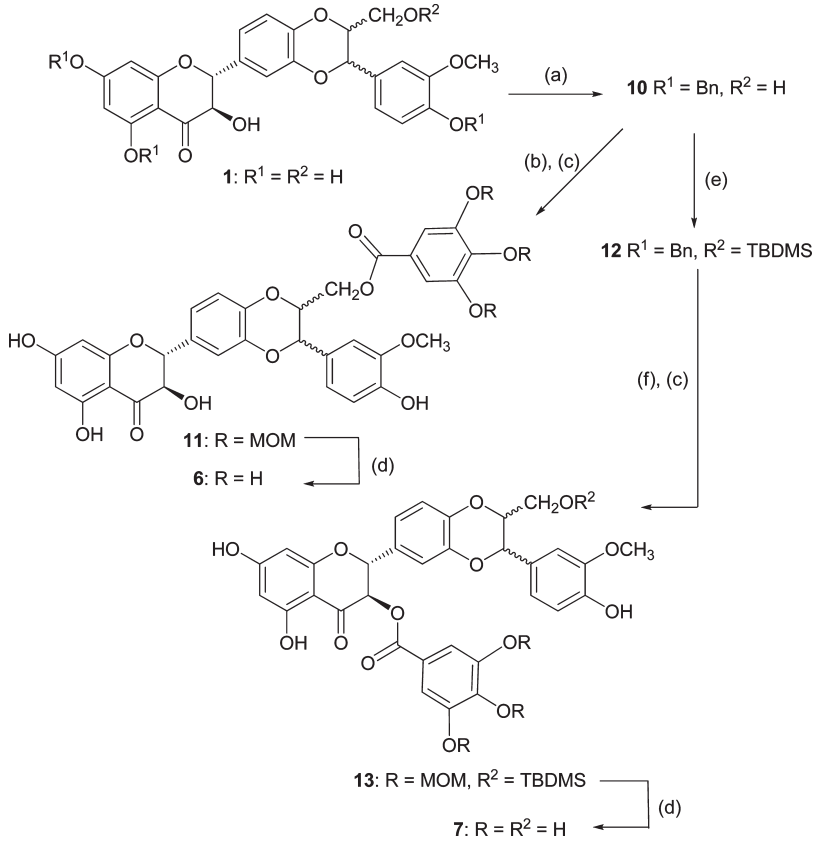

[a] Reagents and conditions: (a) BnBr (5 equiv), NaH (3 equiv), DMF, 0 °C for 1 h, then room temp 1 h;[8] (b) **4** (1.2 equiv), DCC (2 equiv), DMAP (0.5 equiv), CH_2Cl_2, 2 h at 0 °C, 2 h at room temp, 44% (after step c); (c) H_2—Pd/C, AcOEt; (d) HCl (cat.), MeOH, 3 h, 88% from **11**, 83% from **13**; (e) TBDMSCl (1.2 equiv), Py, $AgNO_3$ (cat.), 45 °C, 2 h, 62%; (f) **4** (2 equiv), DCC (2 equiv), DMAP (1 equiv), CH_2Cl_2, 48 h at room temp, 62% (after step c).

purification of the 23-*O*-[3′,4′,5′-tri-*O*-(methoxymethyl)galloyl]-silybin (**11**) easier. Final deprotection of **11** was accomplished by acidic hydrolysis using MeOH/HCl, yielding 23-*O*-gallate **6** (Scheme 2).

The synthesis of 3-*O*-galloylsilybin (**7**) started again from benzylated derivative **10**, which was subsequently protected at the 23-OH with a TBDMS group,[31] yielding compound **12** (Scheme 2). Galloylation of **12** with MOM-protected gallic acid **4** required a substantially longer reaction time than galloylation of the 23-OH (48 h) to achieve sufficient conversion. Two deprotection steps of fully protected intermediate which began with hydrogenolysis of the benzyl groups and was followed by acidic hydrolysis yielded the final 3-*O*-galloylsilybin (**7**). It is worth mentioning that during the attempts to synthesize 20-*O*-galloyl ester starting from 5,7-di-*O*-tritylsilybin (**14**),[32] an exclusive formation of galloyl ester at 3-OH was observed (Scheme 3). Moreover, esterification of the 3-OH proceeds substantially more quickly using **14** than when starting from **12**.

Synthesis of the 20-*O*-gallate **8** was based on the procedure developed for galloylation of the 7-OH, using Et_3N as a base producing phenolate at an appropriate position and thus directed the regioselectivity of esterification. The more reactive 7-OH had to be previously protected with a benzyl group, yielding compound **16** (Scheme 4). Esterification of **16** using acyl chloride **3** and Et_3N led to benzyl-protected ester **17**, which after hydrogenolysis gave 20-*O*-galloylsilybin (**8**) (Scheme 4).

Scheme 3. Alternative Synthesis of 3-*O*-Galloylsilybin (7)[a]

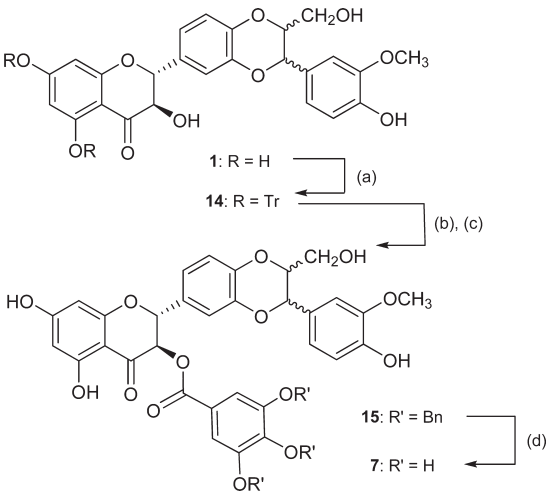

[a] Reagents and conditions: (a) TrCl (2 equiv), Et_3N (3 equiv), CH_2Cl_2, 3 h at room temp;[32] (b) 3,4,5-tri-*O*-benzylgallic acid, DCC/DMAP, CH_2Cl_2; (c) HCl (cat.), MeOH, 3 h, 52% (after two steps); (d) H_2—Pd/C, AcOEt, 12 h, 71%.

Since the starting natural silybin was a nearly equimolar mixture of the A and B isomers, some NMR signals were doubled.

dx.doi.org/10.1021/jm201034h | *J. Med. Chem.* 2011, 54, 7397–7407

The correct proton signal multiplicity was therefore obtained from HOM2DJ and COSY. Fortunately, the chemical shift differences were in the ppb range so that common cross-peaks for both isomers were usually observed in the heterocorrelated experiments. The unambiguous NMR signal assignment is essential for the structure elucidation. Therefore, the measurements were performed in DMSO-d_6, in which the observation of OH signals is possible. The assignment of all hydroxyl groups represents an indirect way of determining the site of substitution (missing signal of OH proton indicates substitution), providing the information on sites that are not affected. Some substituents (OCH_3, OCH_2Ph) offer direct means of their localization: NOE to their neighboring protons (OCH_3), H,H long-range couplings (OCH_3, OCH_2Ph), and $^3J_{C,H}$.

The position of galloyl group in **6** and **7** was determined using downfield acylation shift (H-3 or H-23). The heteronuclear coupling between H-3 or H-23 and the carbonyl of respective acyls was a direct proof of the acylation. An acylation at 7-OH (**5**, **5a**, **5b**, and **9**) can be inferred from chemical shift changes of C-6, C-7, C-8, and C-4a. An acylation at 20-OH (compounds **8** and **17**) was accompanied by corresponding changes of chemical shift of C-19, C-20, and C-21 observable in ^{13}C NMR.

Scheme 4. Synthesis of 20-*O*-Galloylsilybin (8)[a]

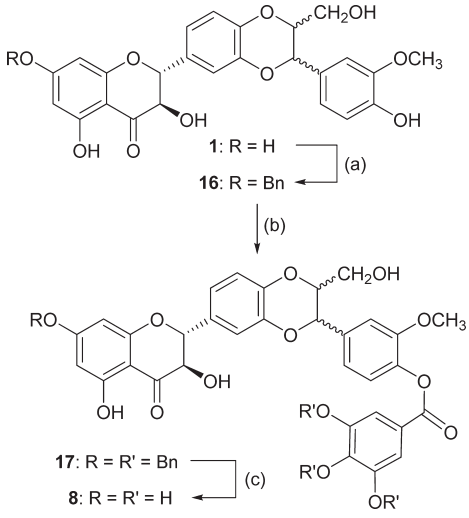

[a] Reagents and conditions: (a) BnBr (2 equiv), K_2CO_3 (7 equiv), acetone, reflux, 3 h;[21] (b) 3,4,5-tri-*O*-benzylgalloyl chloride (**3**, 1.2 equiv), Et_3N (2 equiv), CH_2Cl_2, room temp, 1 h, 39%; (c) H_2—Pd/C, EtOAc, room temp, 12 h, 84%.

BIOLOGICAL RESULTS

Cytotoxicity. All the compounds studied (Figure 2) were first tested for cytotoxicity on HUVEC, measured as the ability to reduce MTT (3-(4,5-dimethyl-2-thiazolyl)-2,5-diphenyl-2*H*-tetrazolium bromide). Silybin was the least toxic, with 50% viability at 72.58 ± 4.18 μM, and 7-*O*-galloylsilybin exhibited the lowest IC_{50} (7.85 ± 0.52 μM for the B stereoisomer; see Table 1). However, unusual behavior with this model was noted for 7-*O*-galloylsilybins, which exhibited approximately 50% viability at all concentrations above their IC_{50}, but even up to 100 μM it did not drop below 40% of the control. At the same time, silybin and its derivatives have limited solubility and concentrations higher than 30 μM are hard to achieve, even in the presence of DMSO. No consistent effect was noted on LDH leakage (data not shown).

Cell Growth Assay. Angiogenesis involves the local proliferation of endothelial cells. We investigated the ability of silybin and its gallates to inhibit the growth of endothelial cells. Table 2 and

Table 1. Effect of Silybin and Its Gallates on Viability of HUVEC[a]

	IC_{50} (μM)
silybin (**1**)	72.58 ± 4.18[a]
silybin A (**1a**)	62.33 ± 2.39[b]
silybin B (**1b**)	60.47 ± 1.03[b]
3-*O*-galloylsilybin (**7**)	64.95 ± 3.59[a,b]
7-*O*-galloylsilybin (**5**)	9.21 ± 0.93[c]
7-*O*-galloylsilybin A (**5a**)	17.14 ± 0.59
7-*O*-galloylsilybin B (**5b**)	7.85 ± 0.52[c]
20-*O*-galloylsilybin (**8**)	35.41 ± 2.10
23-*O*-galloylsilybin (**6**)	55.02 ± 4.21

[a] The cells were grown in 96-well plates to confluency, then incubated with the tested compounds for 16 h. MTT-reducing ability is expressed as IC_{50} (mean ± SD from three independent experiments performed in triplicate). Values marked by the same letter are not significantly different ($p < 0.05$).

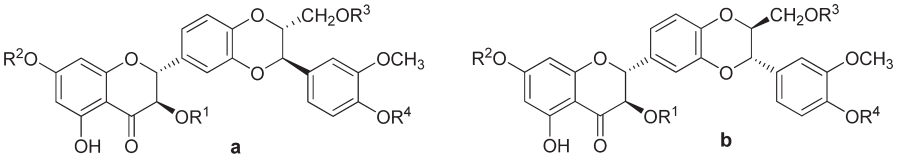

	R^1	R^2	R^3	R^4
1a	H	H	H	H
1b	H	H	H	H
5a	H	Gall	H	H
5b	H	Gall	H	H
5	H	Gall	H	H
6	H	H	Gall	H
7	Gall	H	H	H
8	H	H	H	Gall

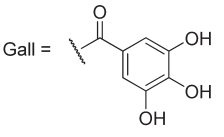

Figure 2. Structures of the silybin gallates tested.

dx.doi.org/10.1021/jm201034h | J. Med. Chem. 2011, 54, 7397–7407

Table 2. Inhibitory Effects of the Studied Compounds on HUVEC Proliferation (MTT Assay)[a]

	IC_{50} (μM)
silybin (**1**)	9.99 ± 0.11^{a}
silybin A (**1a**)	8.83 ± 0.44^{b}
silybin B (**1b**)	6.49 ± 0.33^{c}
3-*O*-galloylsilybin (**7**)	12.31 ± 0.27^{d}
7-*O*-galloylsilybin (**5**)	4.75 ± 0.13^{c}
7-*O*-galloylsilybin A (**5a**)	6.06 ± 0.15^{b}
7-*O*-galloylsilybin B (**5b**)	4.29 ± 0.30^{c}
20-*O*-galloylsilybin (**8**)	$10.35 \pm 0.35^{a,d}$
23-*O*-galloylsilybin (**6**)	11.59 ± 0.71^{d}

[a] HUVECs (4×10^3) in a total volume of 100 μL were incubated with serial dilutions of the tested compounds for 3 days. MTT-reducing ability is expressed as IC_{50} (mean ± SD from three independent experiments performed in triplicate). Values marked by the same letter are not significantly different ($p < 0.05$).

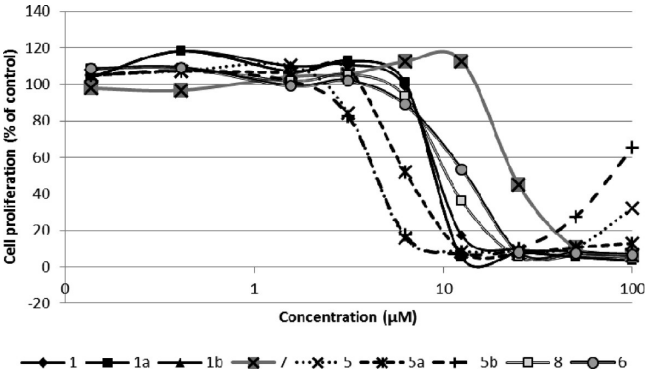

Figure 3. Effect of silybin gallates on HUVEC proliferation. Cell proliferation is presented as a percentage of control cell growth. Each point represents the mean of three independent experiments performed in triplicate. SD values were always below 10% and were omitted for clarity.

Figure 3 show 7-*O*-galloylsilybin and especially its B isomer exerting the most potent inhibitory effect on HUVEC proliferation. Virtual increase in cell proliferation in the presence of very high concentrations of 7-*O*-galloylsilybins as seen in Figure 3 was due to their precipitation in the culture medium and interference with formazan determination.

Endothelial Cell Migration Assay. The results obtained with this assay (Figure 4), following the reoccupation of the "wound" space after overnight (16−20 h) treatment, enabled us to determine the minimal inhibitory concentration (MIC) for each tested compound. These MICs were as follows: for silybin, 50 mM (virtually identical for both isomers); for 3-*O*-galloylsilybin, 50 mM; for 7-*O*-galloylsilybin, 10−20 mM (virtually identical for both isomers); for 20-*O*-galloylsilybin, 20 mM; for 23-*O*-galloylsilybin, 20 mM.

Endothelial Cell Differentiation Assay: Tube Formation on Matrigel. After 6 h of treatment, we only detected a clear inhibitory effect for 7-*O*-galloylsilybin at 50 μM. For the control silybin, this kind of inhibitory effect could not be detected at such a low concentration and it was only observed at 75 μM and above. In extended incubations, after 24 h of treatment we were able to determine the minimal inhibitory concentration (MIC) for each tested compound (those assays where no tubular structure could be observed were considered positive). These MICs were as follows: for silybin, 75 μM; for 3-*O*-galloylsilybin, 75 μM; for 7-*O*-galloylsilybin, 25 μM; for 20-*O*-galloylsilybin, 60 μM; for 23-*O*-galloylsilybin, 75 μM.

Quantification using the angiogenic score enabled us to compare the tested compounds in more detail. In a typical experiment, the angiogenic score in control wells was 3.57 ± 0.64 and decreased to 0.73 ± 0.09 in wells treated with 2-methoxyestradiol (positive control). For 7-*O*-galloylsilybin, significant inhibition of tube formation was already observed at 10 μM (79.9 ± 3.7% of control), and this effect was dose-dependent. When its A and B isomers were evaluated, quite similar results were obtained. In contrast, 3-*O*-galloylsilybin had virtually no effect up to 75 μM and only a very slight (although significant) effect was observed for 23-*O*-galloylsilybin (81.5 ± 15.9% of control at 20 μM) and 20-*O*-galloylsilybin (94.5 ± 4.1% of control at 20 μM and 49.5 ± 2.0% at 30 μM) (Figures 5 and 6). Taken together, these results clearly show that 7-*O*-galloylsilybin is the most potent inhibitor of this key step of angiogenesis.

DISCUSSION

Silybin was recently reported to be a potent antiangiogenic compound with significant effects on various phases of angiogenesis.[16] Moreover, the above-mentioned work only evaluated the antiangiogenic activity of natural silybin (mixture of two diastereomers). The results of our study showed that silybin has rather poor antiangiogenic effects, whereas silybin B is a slightly better inhibitor of angiogenesis than silybin A.

On the basis of the results of our in vitro antiangiogenic assays on HUVEC cells, it has been clearly demonstrated that galloylation of silybin is a suitable way to improve its antiangiogenic effects. This SAR study had two important goals: (i) to determine the most suitable position of the silybin molecule for galloylation; (ii) to evaluate the influence of its stereochemistry on its corresponding biological activity.

As for the position of silybin substitution, we identified two appropriate sites of silybin molecule, i.e., its 7-OH and 20-OH groups, finding the 7-OH to be more suitable. On the other hand, galloylation of aliphatic OH groups was found to have a deleterious effect on the antiangiogenic activity. Surprisingly, 3-*O*-galloylsilybin (**7**) was identified as the least active derivative, even worse than the parent silybin (**1**), despite its highly similar structure compared to *epi*-gallocatechin gallate (Figure 7), the most active antiangiogenic component identified in green tea extracts.[20] Comparison of their structures raises several possible explanations of their contradictory antiangiogenic efficacy: (i) the presence of a coniferyl alcohol moiety in the structure of **7** can lead to the loss of its activity compared to EGCG; (ii) the carbonyl group at the C-4 of **7** causes this ring to be more rigid than in EGCG, which can again lead to lower activity; (iii) most probably, the stereochemistry at C-3 of both compounds could be a critical factor for their activities. It seems that both pyrogallol moieties (B and G rings) present in EGCG have to be in one plane, which is not the case with compound **7**, which is in the trans-configuration at C-2, C-3.

On the basis of the correlation of the structures of galloylsilybins with EGCG, the higher efficacy of both 7-*O*-galloylsilybin (**5**) and 20-*O*-galloylsilybin (**8**) can also be explained. If the coplanarity of the B and G rings serves as a structural motif for the high antiangiogenic activity of EGCG, we can also find similar motifs in the structures of both silybin gallates **5** and **8** (Figure 8).

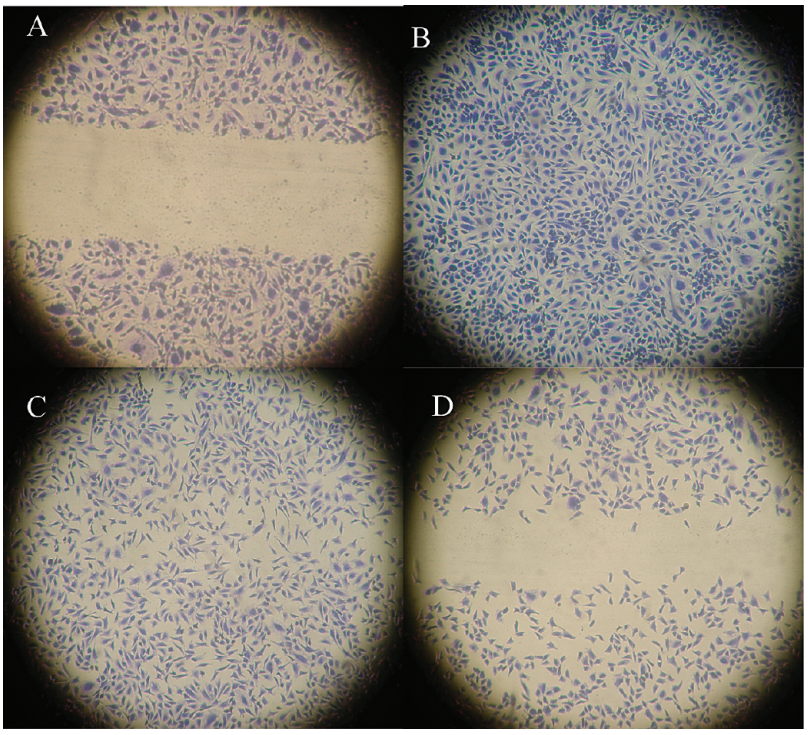

Figure 4. Effect of 7-*O*-galloylsilybin on endothelial cell migration after overnight (16−20 h) incubation in 24-well plates: (A) $T = 0$; (B) control; (C) 7-*O*-galloylsilybin, 10 μM; (D) 7-*O*-galloylsilybin, 20 μM.

As the structural similarity is higher for gallate **5**, it should possess an accordingly higher activity than the rather less similar **8**.

To evaluate the effect of stereochemistry on the antiangiogenic activity, the most active compound from the tested series, 7-*O*-galloylsilybin (**5**), was synthesized from stereochemically pure silybins. Again, the effects of pure B-isomer **5b** were significantly higher than those of **5a**.

MATERIALS AND METHODS

Chemistry. General Methods. Silybin (mixture of A and B, approximately 1:1) was kindly provided by Dr. L. Cvak (TAPI Galena, IVAX Pharmaceuticals, Opava, CZ). 3,4,5-Tri-*O*-benzylgalloyl chloride (**3**) was prepared by reacting 3,4,5-tri-*O*-benzylgallic acid (**2**) with an excess of oxalyl chloride and used immediately after preparation without further purification. All other chemicals were purchased from Sigma-Aldrich and used as obtained. The reactions were monitored by TLC on F_{254} silica gel (Merck), and the spots were visualized with UV light and by charring with 5% H_2SO_4 in EtOH.

NMR spectra were recorded on a Bruker Avance III 400 MHz spectrometer (400.13 MHz for ^{1}H, 100.55 MHz for ^{13}C at 30 °C) and a Bruker Avance III 600 MHz spectrometer (600.23 MHz for ^{1}H, 150.93 MHz for ^{13}C at 30 °C) in DMSO-d_6 (99.9 atom % D, Sigma-Aldrich, Steinheim, Germany). Residual signals of solvent were used as an internal standard (δ_H 2.500 ppm, δ_C 39.60 ppm). All NMR experiments, ^{1}H NMR, ^{13}C NMR, *J*-resolved, COSY, HSQC, HSQC-TOCSY, HMBC, and 1D TOCSY were performed using the manufacturer's software. ^{1}H NMR and ^{13}C NMR spectra were zero filled to 4-fold data points and multiplied by window function before Fourier transformation. The two-parameter double-exponential Lorentz−Gauss function was applied for ^{1}H to improve resolution, and line broadening (1 Hz) was applied to get better ^{13}C signal-to-noise ratio. Chemical shifts are given in δ scale with digital resolution, justifying the reported values to three (δ_H) or two (δ_C) decimal places.

HRMS measurements were performed using a commercial APEX-Ultra FTMS instrument equipped with a 9.4 T superconducting magnet and a dual II ESI/MALDI ion source (Bruker Daltonics, Billerica, MA, U.S.). The analysis was performed using electrospray ionization (ESI), and the spectra were acquired in negative ion mode. The interpretation of mass spectra was done using DataAnalysis, version 4.0, software package (Bruker Daltonics, Billerica, MA, U.S.).

Positive-ion electrospray ionization (ESI) mass spectra were recorded on a LCQDECA spectrometer (ThermoQuest, San Jose, CA, U.S.). HPLC experiments were performed in a Shimadzu Prominence UFLC system (Kyoto, Japan) with a PDA detector connected to a Chromolith Performance RP-18e monolithic column (100 mm × 3 mm i.d.) (Merck, Germany). Purity of the tested compounds was determined using HPLC, and in all cases the purity reached at least 95% (for respective chromatograms see Supporting Information).

Stereochemically pure **1a** and **1b** were prepared using Novozym 435.[7] 5,7,20-Tri-*O*-benzylsilybin (**10**),[8] 7-*O*-benzylsilybin (**16**),[21] 3,4,5-tri-*O*-benzylgallic acid (**2**),[34] and 5,7-di-*O*-tritylsilybin (**14**)[32] were prepared according to published procedures, and their identity was verified by appropriate structural analysis.

3,4,5-Tri-*O*-methoxymethylgallic Acid (4). MOMCl (7.1 mL, 70.109 mmol, 75%) was added dropwise to a cooled solution of gallic acid (3 g, 17.647 mmol) and NaH (3.2 g, 80 mmol, 60% dispersion in min oil w/w) in dry DMF (30 mL). The mixture was stirred for 30 min at 0 °C, then for 12 h at room temperature, diluted with ice-cold water, acidified with an aqueous solution of tartaric acid (pH < 7), and extracted with EtOAc (2 × 75 mL). The organic layers were combined, dried (Na_2SO_4), and evaporated. The crude mixture was dissolved in EtOH (100 mL). Aqueous KOH solution (1 M, 30 mL) was added, and the resulting mixture was stirred for 12 h at room temperature. The reaction mixture was concentrated in vacuo, then poured into ice-cold water and acidified with tartaric acid (pH < 7). The aqueous portion was then extracted with EtOAc (2 × 75 mL), and the organic portion was dried (Na_2SO_4) and evaporated. Flash chromatography ($CHCl_3$/toluene/acetone/HCO_2H,

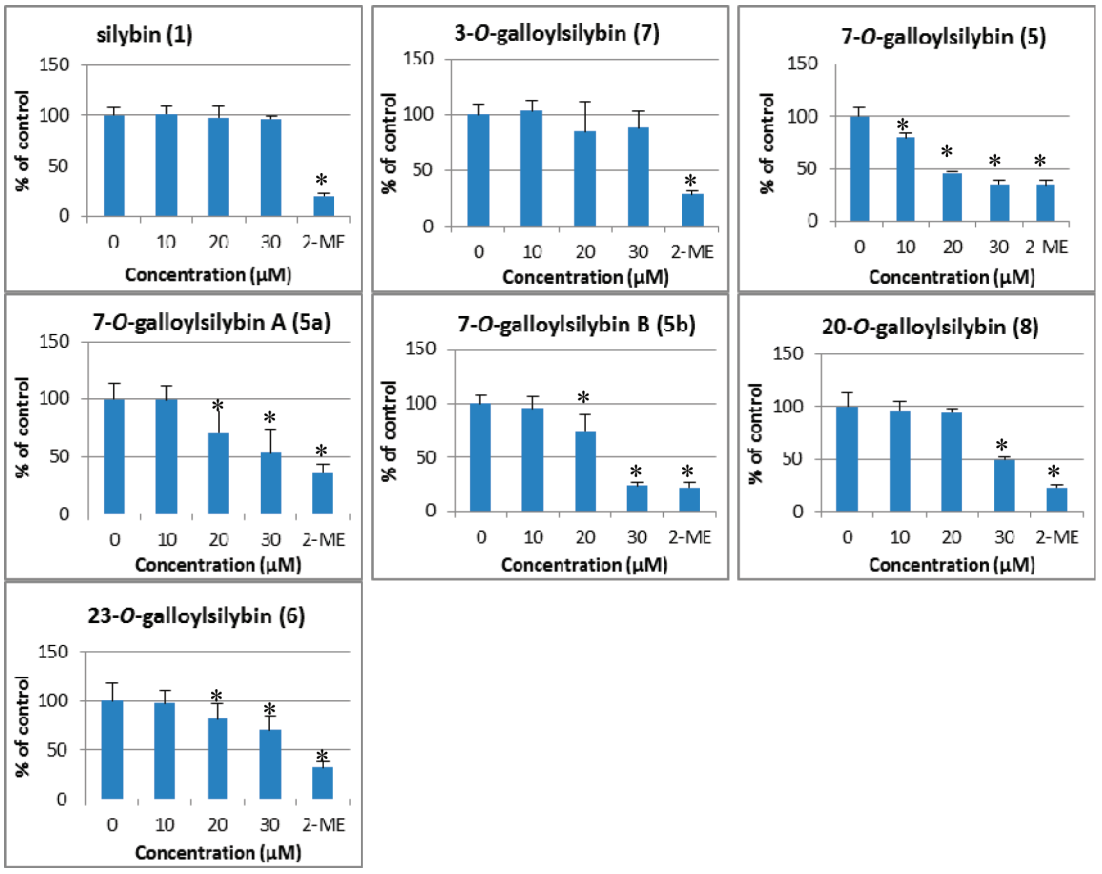

Figure 5. Inhibition of HUVEC tube formation by silybin gallates. HUVECs were incubated overnight on Matrigel in the absence (control) or presence of the tested compounds or 2-methoxyestradiol (2-ME, 10 μM, positive control), and the cultures were observed (40× magnification) and photographed at 3× optical zoom with an Olympus CK40 inverted microscope. Three pictures in total covering the whole area were recorded per well and transferred to the computer for image analysis. The extent of tube formation was quantified using an angiogenic score as proposed recently[33] in a representative optical field containing around 100 cells, and the results were expressed as a percentage of the nontreated control: ∗, $p < 0.05$ compared with nontreated control.

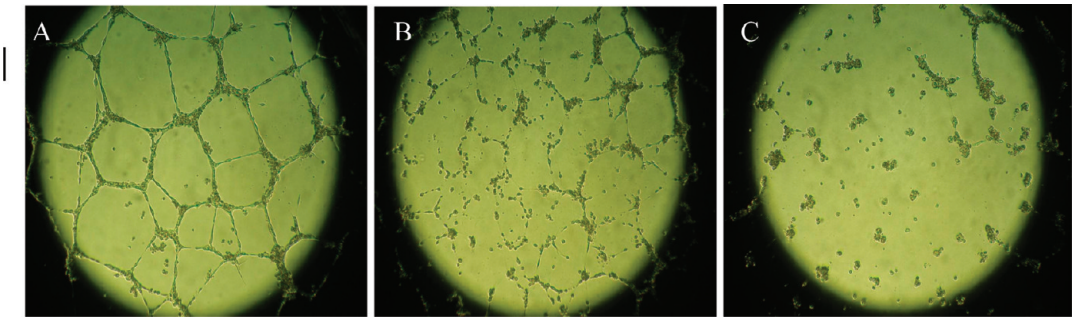

Figure 6. Inhibition of HUVEC tube formation by silybin gallates. HUVECs were incubated overnight on Matrigel in the absence (control) or presence of the tested compounds or 2-methoxyestradiol (2-ME, 10 μM, positive control), and cultures were observed (40× magnification) and photographed at 3× optical zoom with an Olympus inverted microscope CK40: (A) control; (B) 7-*O*-galloylsilybin, 10 μM; (C) 2-ME.

85:10:5:1) yielded title compound **4** (1.8 g, 34%) as a white amorphous solid. ^{1}H NMR (600 MHz) δ 3.413 (6H, s, OMe), 3.506 (3H, s, OMe), 5.127 (2H, s, *p*-OCH_2), 5.236 (4H, s, *m*-OCH_2), 7.395 (2H, s, H-ortho). ^{13}C NMR (150 MHz) δ 55.88 (q, OMe), 56.56 (q, OMe), 94.82 (t, *m*-OCH_2), 97.80 (t, *p*-OCH_2), 110.81 (d, C-ortho), 126.23 (s, C-ipso), 139.96 (s, C-para), 150.39 (s, C-meta), 166.64 (s, *i*-COOH). MS-ESI (m/z): 325 (M^+ + Na).

7-*O*-(3′,4′,5′-Tri-*O*-benzylgalloyl)silybin (9): Method I. Silybin (**1**, 1000 mg, 2.073 mmol), 3,4,5-tri-*O*-benzylgalloyl chloride (**3**) (1140 mg, 2.484 mmol), and DMAP (250 mg, 2.046 mmol) were dissolved in dry pyridine (30 mL), and the mixture was stirred at 0 °C for 1 h. Reaction was stopped by diluting in ice-cold HCl (1 M, 150 mL). The aqueous portion was extracted with EtOAc (2 × 50 mL), and the organic layers were combined, dried (Na_2SO_4), and evaporated. The dry solid left after flash chromatography ($CHCl_3$/acetone/HCO_2H, 95: 5: 1) was the title compound **9** (600 mg, 32%) as a white amorphous solid. MS-ESI (m/z): 927 (M^+ + Na). For ^{1}H and ^{13}C NMR data, see Tables S1 and S2 in the Supporting Information.

dx.doi.org/10.1021/jm201034h |*J. Med. Chem.* 2011, 54, 7397–7407

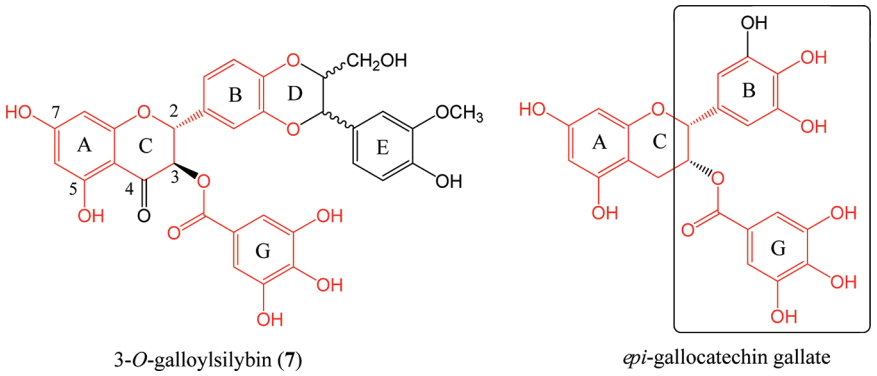

Figure 7. Comparison of structures of the least active silybin derivative and the most active component of green tea extract (congruous parts are highlighted in red).

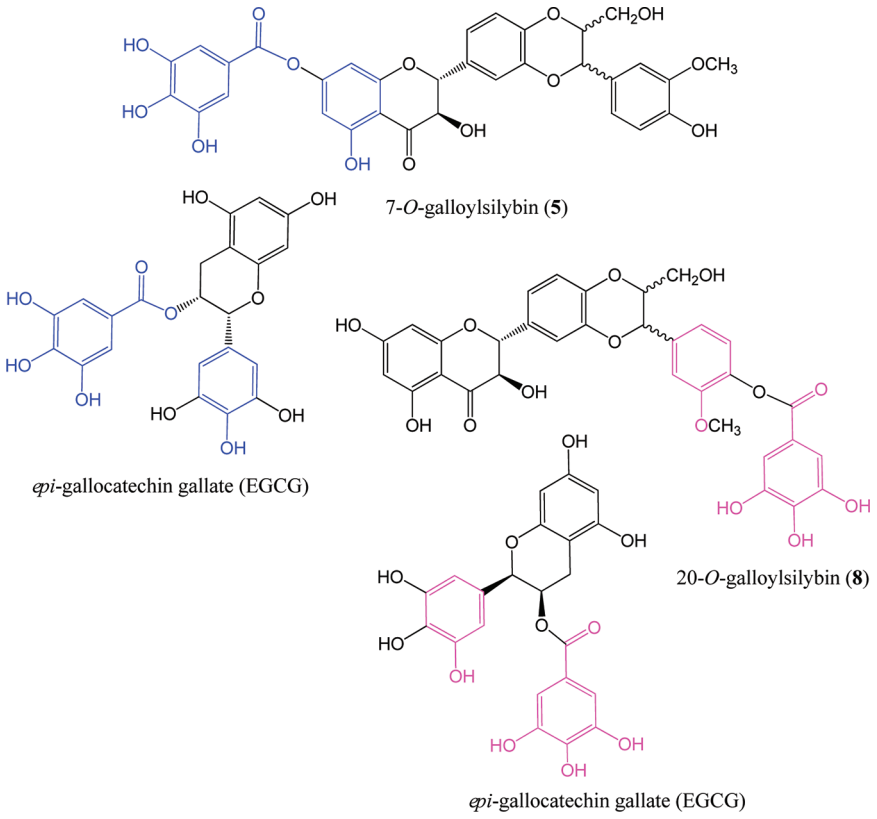

Figure 8. Correlation of the structures of the active galloylsilybins with EGCG (corresponding motifs are highlighted in the same color).

7-*O*-(3′,4′,5′-Tri-*O*-benzylgalloyl)silybin (9): Method II. Et_3N (0.145 mL, 1.042 mmol) was added to a stirred solution of silybin (**1**, 250 mg, 0.518 mmol) in CH_2Cl_2/MeCN (20 mL, 1:3 v/v), and the mixture was stirred at room temperature for 10 min. Then a solution of **3** (287 mg, 0.626 mmol) in CH_2Cl_2 (10 mL) was added dropwise and the resulting mixture was stirred at room temperature for 1 h. Solvents were evaporated to dryness by coevaporation with toluene. The dry solid left after flash chromatography ($CHCl_3$/acetone/HCO_2H, 95:5:1) was the title compound **9** (380 mg, 81%) as a white amorphous solid. MS-ESI (m/z): 927 (M^+ + Na). For ^1H and ^{13}C NMR data, see Tables S1 and S2 in the Supporting Information.

7-*O*-Galloylsilybin (5). Compound **9** (500 mg, 0.553 mmol) was dissolved in EtOAc (30 mL), and then Pd/C (500 mg, 10% Pd) was added. The reaction mixture was stirred under a hydrogen atmosphere for 12 h. The Pd was then removed by filtration through Celite that was washed with acetone, and the solvent was evaporated. The residue left after flash chromatography ($CHCl_3$/acetone/HCO_2H, 5:1:0.1) was the title compound **5** (320 mg, 91%) as a white amorphous solid. HRMS calcd ($M - H^+$) 633.1244, found 633.1243. For ^1H and ^{13}C NMR data, see Tables S1 and S2 in the Supporting Information.

7-*O*-Galloylsilybin A (5a). Compound **5a** was prepared via the same procedure as for **5** (intermediate **9a** was obtained using method II), starting from pure **1a**. HRMS calcd ($M - H^+$) 633.1244, found 633.1243. For ^1H and ^{13}C NMR data, see Tables S1 and S2 in the Supporting Information.

7-*O*-Galloylsilybin B (5b). Compound **5b** was prepared via the same procedure as for **5** (intermediate **9b** was obtained using method II), starting from pure **1b**. HRMS calcd ($M - H^+$) 633.1244, found

dx.doi.org/10.1021/jm201034h |*J. Med. Chem.* 2011, 54, 7397–7407

633.1243. For ^{1}H and ^{13}C NMR data, see Tables S1 and S2 in the Supporting Information.

23-*O*-(3′,4′,5′-Tri-*O*-methoxymethylgalloyl)silybin (11). 5,7,20-Tri-*O*-benzylsilybin (**10**, 900 mg, 1.196 mmol), the acid **4** (434 mg, 1.436 mmol), DCC (494 mg, 2.394 mmol), and DMAP (73 mg, 0.598 mmol) were dissolved in dry CH_2Cl_2 (50 mL), and the mixture was stirred at 0 °C for 2 h and then an additional 2 h at room temperature. The mixture was then evaporated, redissolved in CH_2Cl_2, filtered to remove DCU, and then evaporated. The crude reaction mixture was dissolved in CH_2Cl_2 (6 mL) and then filtered through a pad of silica gel (3 cm). The elution was performed using petroleum ether/EtOAc (1:1, 250 mL). The resulting mixture (1.38 g) was subjected to hydrogenolysis using Pd/C (720 mg, 10% of Pd) in EtOAc (40 mL) for 12 h. Solids were removed by filtration through Celite, which was washed with acetone, and the combined solution was evaporated. Flash chromatography ($CHCl_3$/toluene/acetone/HCO_2H, 95:5:5:1) yielded title compound **11** (400 mg, 44%) as a white amorphous solid. MS-ESI (m/z): 789 (M^+ + Na). For ^{1}H and ^{13}C NMR data, see Tables S1 and S2 in the Supporting Information.

23-*O*-Galloylsilybin (6). HCl (0.2 mL, 36% v/v) was added to a solution of **11** (220 mg, 0.287 mmol) in MeOH (30 mL), and the resulting mixture was stirred at room temperature for 3 h. The reaction was quenched by the addition of saturated $NaHCO_3$ solution (to pH 7), and the solvents were removed by coevaporation with pure EtOH. The solid residue was dissolved in acetone, filtered to remove inorganic salts, and evaporated. Flash chromatography ($CHCl_3$/acetone/HCO_2H, 5:1:0.1) yielded title compound **6** (160 mg, 88%) as a white amorphous solid. HRMS calcd ($M - H^+$) 633.1244, found 633.1243. For ^{1}H and ^{13}C NMR data, see Tables S1 and S2 in the Supporting Information.

5,7,20-Tri-*O*-benzyl-23-*O*-(*tert*-butyldimethylsilyl)silybin (12). Powdered $AgNO_3$ (359 mg, 2.113 mmol) was added to a solution of 5,7,20-tri-*O*-benzylsilybin (**10**, 1590 mg, 2.112 mmol) and TBDMSCl (382 mg, 2.534 mmol) in dry pyridine (15 mL), and the mixture was stirred at 45 °C for 2 h. The mixture was then diluted with ice-cold water. The precipitate was filtered off and dissolved with EtOAc. The organic phase was dried over anhydrous Na_2SO_4 and evaporated to dryness. Flash chromatography (petroleum ether/EtOAc, 3:1) yielded title compound **12** (1130 mg, 62%) as a white amorphous solid. MS-ESI (m/z): 889 (M^+ + Na). For ^{1}H and ^{13}C NMR data, see Tables S1 and S2 in the Supporting Information.

23-*O*-*tert*-Butyldimethylsilyl-3-*O*-[(3′,4′,5′-tri-*O*-methoxymethyl)galloyl]silybin (13). Compound **12** (500 mg, 0.577 mmol), 3,4,5-tri-*O*-methoxymethylgallic acid (**4**, 349 mg, 1.153 mmol), DCC (238 mg, 1.153 mmol), and DMAP (70 mg, 0.577 mmol) were dissolved in dry CH_2Cl_2 (30 mL), and the mixture was stirred at room temperature for 48 h. The mixture was then evaporated, redissolved in CH_2Cl_2 (10 mL), filtered to remove DCU through a pad of silica gel (3 cm), eluted with petroleum ether/EtOAc (1:1, 250 mL), and evaporated. The resulting mixture (920 mg) was subjected to hydrogenolysis (Pd/C, 500 mg, 10% of Pd) in EtOAc (30 mL) for 12 h. The catalyst was removed by filtration through Celite. The Celite pad was washed with acetone, and the solvent was evaporated. Flash chromatography ($CHCl_3$/toluene/acetone/HCO_2H, 95:10:5:1) yielded title compound **13** (315 mg, 62%) as a white amorphous solid. MS-ESI (m/z): 903 (M^+ + Na). For ^{1}H and ^{13}C NMR data, see Tables S1 and S2 in the Supporting Information.

3-*O*-Galloylsilybin (7): Method I. HCl (0.5 mL, 36% v/v) was added to a solution of **13** (200 mg, 0.287 mmol) in MeOH (10 mL), and the reaction mixture was stirred at room temperature for 3 h. After the reaction was quenched with saturated $NaHCO_3$ solution (to neutral pH), the solvents were removed by coevaporation with absolute EtOH. The solid residue was dissolved in acetone, filtered, and evaporated. Flash chromatography ($CHCl_3$/acetone/HCO_2H, 5:1:0.1) yielded title compound **7** (120 mg, 83%) as a white amorphous solid. HRMS calcd ($M - H^+$) 633.1244, found 633.1244. For ^{1}H and ^{13}C NMR data, see Tables S1 and S2 in the Supporting Information.

3-*O*-Galloylsilybin (7): Method II. 5,7-Di-*O*-tritylsilybin (**14**, 470 mg, 0.487 mmol), 3,4,5-tri-*O*-benzylgallic acid (**2**, 257 mg, 0.584 mmol), DCC (201 mg, 0.974 mmol), and DMAP (59 mg, 0.483 mmol) were dissolved in dry CH_2Cl_2 (25 mL), and the mixture was stirred at room temperature for 1 h. MeOH (25 mL) and HCl (1 mL, 36% v/v) were then added, and the resulting mixture was stirred for another 2 h. Reaction was stopped by the addition of saturated $NaHCO_3$ solution to neutral pH. The mixture was evaporated to dryness by coevaporation with toluene, redissolved in CH_2Cl_2, and filtered. Flash chromatography ($CHCl_3$/toluene/acetone/HCO_2H, 95:5:5:1) yielded 3-*O*-[(3′,4′,5′-tri-*O*-benzyl)galloyl]silybin (**15**, 230 mg, 52%) as a white amorphous solid. MS-ESI (m/z): 927 (M^+ + Na). For ^{1}H and ^{13}C NMR data, see Tables S1 and S2 of Supporting Information.

Hydrogenolysis of **15** (200 mg, 0.221 mmol) with Pd/C (100 mg, 10% w/w) in EtOAc (15 mL) for 12 h yielded crude title compound **7**, which was purified by flash chromatography ($CHCl_3$/acetone/HCO_2H, 5:1:0.1) to yield pure **7** (99 mg, 71%) as a white amorphous solid. HRMS calcd ($M - H^+$) 633.1244, found 633.1244. For ^{1}H and ^{13}C NMR data, see Tables S1 and S2 in the Supporting Information.

7-*O*-Benzyl-20-*O*-[(3′,4′,5′-tri-*O*-benzyl)galloyl]silybin (17). Et_3N (0.243 mL, 1.748 mmol) was added to a stirred solution of **16** (500 mg, 0.874 mmol) in CH_2Cl_2 (50 mL), and the mixture was stirred at room temperature for 10 min. A solution of **3** (441 mg, 0.962 mmol) in CH_2Cl_2 (10 mL) was then added dropwise, and the resulting mixture was stirred at room temperature for 1 h. Solvents were evaporated to dryness by coevaporation with toluene. The dry solid left after flash chromatography ($CHCl_3$/toluene/acetone/HCO_2H, 95:10:5:1) was the title compound **17** (343 mg, 39%) as a white amorphous solid. MS-ESI (m/z): 1017 (M^+ + Na). For ^{1}H and ^{13}C NMR data, see Tables S1 and S2 in the Supporting Information.

20-*O*-Galloylsilybin (8). Hydrogenolysis of **17** (300 mg, 0.302 mmol) with Pd/C (200 mg, 10% w/w) in EtOAc (30 mL) for 12 h yielded crude title compound **8**, which was purified by flash chromatography ($CHCl_3$/acetone/HCO_2H, 5:1:0.1) to yield pure **8** (160 mg, 84%) as a white amorphous solid. HRMS calcd ($M - H^+$) 633.1244, found 633.1242. For ^{1}H and ^{13}C NMR data, see Tables S1 and S2 in the Supporting Information.

Biological Testing. Reagents. Dimethylsulfoxide (DMSO) for cell cultures, 2-ME (2-methoxyestradiol), MTT (3-(4,5-dimethyl-2-thiazolyl)-2,5-diphenyl-2*H*-tetrazolium bromide), and fetal calf serum were purchased from Sigma-Aldrich Ltd., U.S. Collagenase was from Serva, Germany. Endothelial cell basal medium with growth factors (endothelial growth medium, EGM) was from Promocell, Germany. Other chemicals and solvents were of analytical grade from Pliva-Lachema, Czech Republic. The tested compounds were dissolved in DMSO at 10 mM, and these stock solutions were kept at −20 °C.

Human Umbilical Vein Endothelial Cells (HUVECs). HUVECs were obtained from human umbilical cords of healthy nonsmoker women (18−35 years) at the Department of Obstetrics and Gynecology, University Hospital in Olomouc, Czech Republic. All volunteers had to fulfill the requirements for study submission and sign a personal awareness declaration. The choice of volunteers was in accordance with the principles of the International Ethics Committee for Biomedical Research (CIOMS, Geneva, 1993), and the study was approved by the Ethic Commission FNO and LF UP. After delivery, part of the umbilical cord (minimum 100 mm) was cut off and placed in sterile Earle's balanced salt supplemented with antibiotics at 4 °C. Endothelial cells were isolated by collagenase digestion up to 20 h after removal. The umbilical cord was washed with EBS and infused with a solution of collagenase in EBS. After incubation (30 min, 37 °C) the cord was washed with Hanks buffer without Ca^{2+} or Mg^{2+}. The cells were cultivated in EGM and used in passages 2−6.

Cytotoxicity. HUVECs were plated on gelatin-coated 96-well cell culture plates in EGM and grown to confluency. The tested compounds were placed in fresh EGM in serial dilutions (100 μL/well) and

incubated overnight (16−20 h). After incubation, 50 μL of medium was removed for determining LDH leakage[35] and 50 μL of fresh medium containing 1 mg/mL of MTT was added.[36] The plates were incubated for a further 3 h (37 °C). The resulting formazan was dissolved in 50 μL of 1% NH_3 in DMSO, and absorbance was read at 540 nm.

Cell Growth Assay. 4×10^3 HUVECs in a total volume of 100 μL were incubated with serial dilutions of the tested compounds for 3 days. After incubation, an amount of 10 μL of MTT (5 mg/mL) was added and the remainder of the method was the same as for the cytotoxicity assay.

Endothelial Cell Migration Assay. The migratory activity of HUVECs was assessed using a wound migratory activity.[37] Confluent monolayers in 24-well cell culture plates were wounded with pipet tips (10−200 μL), giving rise to one acellular 1-mm-wide line per well. After the cells were washed twice with PBS, the cells were supplied with 500 μL of fresh EGM in the absence (controls) or presence of tested compounds. Wounded areas were observed (40× magnification) and photographed at 3× optical zoom with an Olympus inverted microscope CK40 at time zero and after overnight incubation at 37 °C.

Endothelial Cell Differentiation Assay: Tube Formation on Matrigel. An amount of 10 μL of Matrigel (9 mg/mL, BD Biosciences) was applied to the inner well of a μ-Slide Angiogenesis (ibidi) at 4 °C and allowed to polymerize at 37 °C for a minimum of 30 min. Approximately 1×10^4 HUVECs were added to 50 μL of EGM in the absence (control) or presence of the tested compounds or 2-methoxyestradiol (10 μM, positive control). The mixture was incubated overnight, and cultures were observed (40× magnification) and photographed at 3× optical zoom with an Olympus CK40 inverted microscope. Three pictures, in total covering the whole area, were recorded per well and transferred to the computer for image analysis. The extent of tube formation was quantified using an angiogenic score as proposed recently[33] in a representative optical field containing approximately 100 cells, and the results were expressed as a percentage of the nontreated control:

$$\text{angiogenic score} = \left[\frac{\text{No}_s \times 1 + \text{No}_c \times 2 + \text{No}_p \times 3}{\text{No}_t}\right] \pm [0,\ 1,\ \text{or}\ 2]$$

where No_s is the number of sprouting cells, No_c is the number of connected cells, No_p is the number of polygons, and No_t is the total number of cells. The presence of complex mesh (luminal structures consisting of walls two to three cells thick) is given a score of 1 and is added once per optical field. If the wall is four or more cells thick, a score of 2 is awarded.[33]

Statistical Analysis. Data were analyzed with one-way ANOVA using Statext, version 1.4.2b, statistical package. Differences were considered statistically significant when $p < 0.05$. IC_{50} values were obtained using Microsoft Excel 2007.

CONCLUSIONS

This study of the antiangiogenic effects of regioisomeric monogalloyl esters of the flavonolignan silybin provides clear proof that this natural compound is a useful lead structure for relatively simple semisynthetic modifications leading to potent biologically active drugs. A SAR study of the corresponding silybin gallates showed that the position of silybin substitution plays a key role in the activity of the resulting galloyl ester. Accordingly, galloylation of the phenolic OH groups at C-7 or C-20 resulted in rather effective inhibitors of angiogenesis, whereas esterification of the aliphatic OH groups at C-3 and C-23 is connected with a very slight improvement in activity or even loss of activity with the 3-*O*-gallate **7**.

The most effective compound from the series, 7-*O*-gallate **5**, was also prepared from stereochemically pure silybins A and B instead of natural silybin consisting of an equimolar mixture of these two stereoisomers. Evaluation of their antiangiogenic effects clearly showed that the gallate prepared from the B-isomer (**5b**) is significantly more effective than the corresponding A-isomer **5a**. To the best of our knowledge, this is the first study of the antiangiogenic activities of silybin gallates, including their synthesis and the synthesis of stereochemically pure 7-*O*-galloylsilybins A and B. Moreover, this study is one of relatively few studies of the biological activities of stereochemically pure silybins and even fewer studies of the effects of stereochemically pure silybin derivatives.

ASSOCIATED CONTENT

Supporting Information. HPLC chromatograms and HRMS spectra of studied compounds (**5**−**8**, including **5a** and **5b**) and ^1H and ^{13}C NMR data and spectra of compounds **4**−**17**. This material is available free of charge via the Internet at http://pubs.acs.org.

AUTHOR INFORMATION

Corresponding Author

*Phone: (+420) 296 442 510. Fax: (+420) 296 442 509. E-mail: kren@biomed.cas.cz.

ACKNOWLEDGMENT

This work was supported by Grant P207/10/0288 (R.G.) and Grant P301/11/0767 (V.K. and J.U.) from the Czech Science Foundation, Grant MSM 6198959216 (K.V. and J.U.) and Grant OC08049 (V.K.) from the Ministry of Education of the Czech Republic, Research Concept of the Institute of Microbiology Grant AV0Z50200510, Grant PS09/02216 (M.A.M.) from the Spanish Ministry of Science and Innovation, Grant PIE P08-CTS-3759 (M.A.M.) from the Andalusian Government, and ESF COST CM0602 projects. Dr. P. Novák (Institute of Microbiology, Prague, Czech Republich) is thanked for ESI MS and FT MS measurements. We also thank to Casimiro Cárdenas (University of Málaga) for skillful technical assistance.

ABBREVIATIONS USED

HUVEC, human umbilical vein endothelial cell; SAR, structure−activity relationship; EGCG, *epi*-gallocatechin gallate; HOM2DJ, homo-*J*-related hydrogen-1 to hydrogen-1; MTT, 3-(4,5-dimethyl-2-thiazolyl)-2,5-diphenyl-2*H*-tetrazolium bromide; LDH, lactate dehydrogenase; 2-ME, 2-methoxyestradiol; HSQC, heteronuclear single quantum coherence; TOCSY, total correlation spectroscopy; HMBC, heteronuclear multiple bond correlation

REFERENCES

(1) Gažák, R.; Walterová, D.; Křen, V. Silybin and silymarin: new and emerging applications in medicine. *Curr. Med. Chem.* **2007**, *14*, 315–338.

(2) Lee, D. Y.-W.; Liu, Y. Molecular structure and stereochemistry of silybin A, silybin B, isosilybin A, and isosilybin B, isolated from *Silybum marianum* (milk thistle). *J. Nat. Prod.* **2003**, *66*, 1171–1174.

(3) Kim, N.-C.; Graf, T. N.; Sparacino, C. M.; Wani, M. C.; Wall, M. E. Complete isolation and characterization of silybins and isosilybins from milk thistle (*Silybum marianum*). *Org. Biomol. Chem.* **2003**, *1*, 1684–1689.

(4) Ding, T.-M.; Tian, S.-J.; Zhang, Z.-X.; Gu, D.-Z.; Chen, Y.-F.; Shi, Y.-H.; Sun, Z.-P. Determination of active component in silymarin by RP-LC and LC/MS. *J. Pharm. Biomed. Anal.* **2001**, *26*, 155–161.

(5) Marhol, P.; Gažák, R.; Bednář, P.; Křen, V. Narrow-bore core−shell particles and monolithic columns in the analysis of silybin diastereoisomers. *J. Sep. Sci.* **2011**, *34*, 2206–2213.

(6) Monti, D.; Gažák, R.; Marhol, P.; Biedermann, D.; Purchartová, K.; Fedrigo, M.; Riva, S.; Křen, V. Enzymatic kinetic resolution of silybin diastereoisomers. *J. Nat. Prod.* **2010**, *73*, 613–619.

(7) Gažák, R.; Marhol, P.; Purchartová, K.; Monti, D.; Biedermann, D.; Riva, S.; Cvak, L.; Křen, V. Large-scale separation of silybin diastereoisomers using lipases. *Process Biochem.* **2010**, *45*, 1657–1663.

(8) Trouillas, P.; Marsal, P.; Svobodová, A.; Vostálová, J.; Gažák, R.; Hrbáč, J.; Sedmera, P.; Křen, V.; Lazzaroni, R.; Duroux, J.-L.; Walterová, D. Mechanism of the antioxidant action of silybin and 2,3-dehydrosilybin flavonolignans: a joint experimental and theoretical study. *J. Phys. Chem. A* **2008**, *112*, 1054–1063.

(9) Gažák, R.; Sedmera, P.; Vrbacký, M.; Vostálová, J.; Drahota, Z.; Marhol, P.; Walterová, D.; Křen, V. Molecular mechanisms of silybin and 2,3-dehydrosilybin antiradical activity: role of individual hydroxyl groups. *Free Radical Biol. Med.* **2009**, *46*, 745–758.

(10) Payer, B. A.; Reiberger, T.; Rutter, K.; Beinhardt, S.; Staettermayer, A. F.; Peck-Radosavljevic, M.; Ferenci, P. Successful HCV eradication and inhibition of HIV replication by intravenous silibinin in an HIV−HCV coinfected patient. *J. Clin. Virol.* **2010**, *49*, 131–133.

(11) Agarwal, R.; Agarwal, Ch.; Ichikawa, H.; Singh, R. P.; Aggarwal, B. B. Anticancer potential of silymarin: from bench to bed side. *Anticancer Res.* **2006**, *26*, 4457–4498.

(12) Singh, R. P.; Raina, K.; Sharma, G.; Agarwal, R. Silybin inhibits established prostate tumor growth, progression, invasion, and metastasis and suppresses tumor angiogenesis and epithelial−mesenchymal transition in transgenic adenocarcinoma of the mouse prostate model mice. *Clin. Cancer Res.* **2008**, *14*, 7773–7780.

(13) Mateen, S.; Tyagi, A.; Agarwal, C.; Singh, R. P.; Agarwal, R. Silibinin inhibits human nonsmall cell lung cancer cell growth through cell-cycle arrest by modulating expression and function of key cell-cycle regulators. *Mol. Carcinog.* **2010**, *49*, 247–258.

(14) Velmurugan, B.; Gangar, S. C.; Kaur, M.; Tyagi, A.; Deep, G.; Agarwal, R. Silibinin exerts sustained growth suppressive effect against human colon carcinoma SW480 xenograft by targeting multiple signaling molecules. *Pharm. Res.* **2010**, *27*, 2085–2097.

(15) Deep, G.; Agarwal, R. Antimetastatic efficacy of silibinin: molecular mechanisms and therapeutic potential against cancer. *Cancer Metastasis Rev.* **2010**, *29*, 447–463.

(16) Singh, R. P.; Dhanalakshmi, S.; Agarwal, C.; Agarwal, R. Silibinin strongly inhibits growth and survival of human endothelial cells via cell cycle arrest and downregulation of survivin, Akt and NF-kappaB: implications for angioprevention and antiangiogenic therapy. *Oncogene* **2005**, *24*, 1188–1202.

(17) Plíšková, M.; Vondráček, J.; Křen, V.; Gažák, R.; Sedmera, P.; Walterová, D.; Psotová, J.; Šimánek, V.; Machala, M. Effects of silymarin flavonolignans and synthetic silybin derivatives on estrogen and aryl hydrocarbon receptor activation. *Toxicology* **2005**, *215*, 80–89.

(18) Davis-Searles, P. R.; Nakanishi, Y.; Kim, N.-Ch.; Graf, T. N.; Oberlies, N. H.; Wani, M. C.; Wall, M. E.; Agarwal, R.; Kroll, D. J. Milk thistle and prostate cancer: differential effects of pure flavonolignans from *Silybum marianum* on antiproliferative end points in human prostate carcinoma cells. *Cancer Res.* **2005**, *65*, 4448–4457.

(19) Deep, G.; Oberlies, N. H.; Kroll, D. J.; Agarwal, R. Identifying the differential effects of silymarin constituents on cell growth and cell cycle regulatory molecules in human prostate cancer cells. *Int. J. Cancer* **2008**, *123*, 41–50.

(20) Kondo, T.; Ohta, T.; Igura, K.; Hara, Y.; Kaji, K. Tea catechins inhibit angiogenesis in vitro, measured by human endothelial cell growth, migration and tube formation, through inhibition of VEGF receptor binding. *Cancer Lett.* **2002**, *180*, 139–144.

(21) Džubák, P.; Hajdúch, M.; Gažák, R.; Walterová, D.; Svobodová, A.; Psotová, J.; Sedmera, P.; Křen, V. New derivatives of silybin and 2,3-dehydrosilybin and their cytotoxic and P-glycoprotein modulatory activity. *Bioorg. Med. Chem.* **2006**, *14*, 3793–3810.

(22) Gažák, R.; Purchartová, K.; Marhol, P.; Živná, L.; Sedmera, P.; Valentová, K.; Kato, N.; Matsumura, H.; Kaihatsu, K.; Křen, V. Antioxidant and antiviral activities of silybin fatty acid conjugates. *Eur. J. Med. Chem.* **2010**, *45*, 1059–1067.

(23) Wang, F.; Huang, K.; Yang, L.; Gong, J.; Tao, Q.; Li, H.; Zeng, S.; Wu, X.; Stöckigt, J.; Li, X.; Qu, J.; Zhao, Y. Preparation of C-23 esterified silybin derivatives and evaluation of their lipid peroxidation inhibitory and DNA protective properties. *Bioorg. Med. Chem.* **2009**, *17*, 6380–6389.

(24) Theodosiou, E.; Katsoura, M. H.; Loutrari, H.; Purchartová, K.; Křen, V.; Kolisis, F. N.; Stamatis, H. Enzymatic preparation of acylated derivatives of silybin in organic and ionic liquid media and evaluation of their antitumor proliferative activity. *Biocatal. Biotransform.* **2009**, *27*, 161–169.

(25) Ardhaoui, M.; Falcimaigne, A.; Engasser, J. M.; Moussou, P.; Pauly, G.; Ghoul, M. Enzymatic synthesis of new aromatic and aliphatic esters of flavonoids using *Candida antarctica* lipase as biocatalyst. *Biocatal. Biotransform.* **2004**, *22*, 253–259.

(26) Guyot, B.; Bosquette, B.; Pina, M.; Graille, J. Esterification of phenolic acids from green coffee with an immobilized lipase from *Candida antarctica* in solvent-free medium. *Biotechnol. Lett.* **1997**, *19*, 529–532.

(27) Kodera, Y.; Takahashi, K.; Nishimura, H.; Matshushima, A.; Saito, Y.; Inada, Y. Ester synthesis from substituted carboxylic acid catalyzed by polyethylene glycol-modified lipase from *Candida cylindracea* in benzene. *Biotechnol. Lett.* **1986**, *8*, 881–884.

(28) Otto, R. T.; Scheib, H.; Bornscheuer, U. T.; Pleiss, J.; Syldatk, C.; Schmid, R. D. Substrate specificity of lipase B from *Candida antarctica* in the synthesis of aryl-aliphatic glycolipids. *J. Mol. Catal. B: Enzym.* **2000**, *8*, 201–211.

(29) Shintre, M. S.; Ghadge, R. S.; Sawant, S. B. Lipolase catalysed synthesis of benzyl esters of fatty acids. *Biochem. Eng. J.* **2002**, *12*, 131–141.

(30) Takahashi, K.; Yoshimoto, T.; Ajima, A.; Tamaura, Y.; Inada, Y. Modified lipoprotein lipase catalyzes ester synthesis in benzene. Substrate specificity. *Enzyme* **1984**, *32*, 235–240.

(31) Gažák, R.; Svobodová, A.; Psotová, J.; Sedmera, P.; Přikrylová, V.; Walterová, D.; Křen, V. Oxidised derivatives of silybin and their antiradical and antioxidant activity. *Bioorg. Med. Chem.* **2004**, *12*, 5677–5687.

(32) Lee, D. Y. W.; Zhang, X.; Ji, X. S. Preparation of tritium-labeled silybin-A protectant for common liver diseases. *J. Labelled Compd. Radiopharm.* **2006**, *49*, 1125–1130.

(33) Aranda, E.; Owen, G. I. A semi-quantitative assay to screen for angiogenic compounds and compounds with angiogenic potential using the EA.hy926 endothelial cell line. *Biol. Res.* **2009**, *42*, 377–389.

(34) Dehmlow, C.; Murawski, N.; de Groot, H. Scavenging of reactive oxygen species and inhibition of arachidonic acid metabolism by silibinin in human cells. *Life Sci.* **1996**, *58*, 1591–1600.

(35) Bergmeyer, H. U.; Bernt, E. *Lactate Dehydrogenase: UV-Assay with Pyruvate and NADH*; Academic Press: New York and London, 1974.

(36) Sieuwerts, A. M.; Klijn, J. G. M.; Peters, H. A.; Foekens, J. A. The MTT tetrazolium salt assay scrutinized. How to use this assay reliably to measure metabolic-activity of cell-cultures in-vitro for the assessment of growth-characteristics, IC50-values and cell-survival. *Eur. J. Clin. Chem. Clin. Biochem.* **1995**, *33*, 813–823.

(37) Martinez-Poveda, B.; Quesada, A. R.; Medina, M. A. Hypericin in the dark inhibits key steps of angiogenesis in vitro. *Eur. J. Pharmacol.* **2005**, *516*, 97–103.